

Nonlocality in mesoscopic Josephson junctions with strip geometry

Urs Ledermann, Alban L. Fauchère, and Gianni Blatter

Theoretische Physik, Eidgenössische Technische Hochschule, CH-8093 Zürich, Switzerland

(Received 10 December 1998)

We study the current in a clean superconductor–normal-metal–superconductor junction of length d and width w in the presence of an applied magnetic field H . We show that both the geometrical pattern of the current density and the critical current $I_c(\Phi)$, where Φ is the total flux in the junction, depend on the ratio of the Josephson vortex distance $a_0 = \Phi_0/Hd$ and the range $r \sim \sqrt{d\xi_N}$ of the nonlocal electrodynamics [$\Phi_0 = hc/2e$, $\xi_N = \hbar v_F/2\pi T$, and $r(T \rightarrow 0) \sim d$]. In particular, the critical current has the periodicity of the superconducting flux quantum Φ_0 only for $r < a_0$ and becomes, due to boundary effects, $2\Phi_0$ (pseudo)periodic for strong nonlocality, $r > a_0$. Comparing our results to recent experiments of Heida *et al.* [Phys. Rev. B **57**, R5618 (1998)] we find good agreement. [S0163-1829(99)50414-1]

Quantum-mechanical interference effects render the electrodynamics of mesoscopic samples *nonlocal*. In particular, nonlocality is a key element entering the understanding of the magnetic response and the transport in SNS junctions (*s*-wave-superconductor–normal-metal–*s*-wave-superconductor junctions) and SN-proximity sandwiches. The strength and relevance of the nonlocality in general depends on the dimensions of the system, the normal-metal coherence length $\xi_N = \hbar v_F/2\pi T$, and the elastic-scattering length.^{1–3} In this paper we show how the different length scales enter the magnetotransport problem of a mesoscopic SNS junction to produce a shift in the (pseudo)periodicity of the critical current from Φ_0 to $2\Phi_0$.

After the discovery of the Josephson effect in *s*-wave-superconductor–insulator–*s*-wave-superconductor (SIS) tunnel junctions,⁴ interest turned to metallic links of the SNS type,⁵ where the current is conveniently described in terms of Andreev states trapped within the normal-metal region.⁶ For a wide junction, the current density and the supercurrent in the presence of a magnetic field H have been calculated by Antsygina *et al.*,⁷ who found a Φ_0 periodicity in the critical current. Continuous progress in nanofabrication technology made it possible to investigate mesoscopic superconductor-semiconductor heterostructures; see Ref. 8 for a study of the fluctuations in the critical current and its quantization in a superconducting quantum point contact. Recently, Heida *et al.*,⁹ investigating S-2DEG-S junctions (*s*-wave-superconductor–two-dimensional-electron-gas–*s*-wave-superconductor junctions) of comparable width w and length d , have measured a $2\Phi_0$ periodicity of the critical current instead of the standard Φ_0 . A first attempt to explain this finding is due to Barzykin and Zagoskin.¹⁰ Considering the point-contact geometry of Fig. 1(a) with open boundary condition in the metal, they indeed recover a $2\Phi_0$ periodicity in the limit $w/d \rightarrow 0$. However, the experiment of Heida *et al.*⁹ is carried out in the strip geometry of Fig. 1(b) and involves dimensions $w \sim d$ of the same order. In the present paper, we determine the critical current I_c through a clean SNS junction in the presence of an applied magnetic field H , taking proper account of the reflecting boundaries in the normal-metal characteristic for the strip geometry of Fig. 1(b).

We find that the periodicity of the critical current changes from Φ_0 to $2\Phi_0$ as the flux through the junction increases. At low temperatures the crossover to the $2\Phi_0$ periodic current appears at a flux $\sim \Phi_0 w/d$, thus explaining the result of Heida *et al.*,⁹ who found a $2\Phi_0$ periodic pattern for all fields in devices with $w/d \sim 1$.

In our derivation, we neglect screening effects by the induced supercurrent, which is justified as long as $H > \sqrt{8\Phi_0 j_c / cd'}$, where j_c denotes the critical current density of the junction and $d' = d + 2\lambda$ with λ the penetration depth of the two bulk superconductors.¹¹ Since all the length scales in our system (the dimensions w and d , the normal-metal coherence length ξ_N) are much larger than the Fermi wavelength λ_F , we base our calculations on the Eilenberger equations¹² for the quasiclassical Green's functions and extract the current density in the standard way.³

The SNS junction we study is sketched in Fig. 1. In the quasiclassical formulation, the current density in a point P

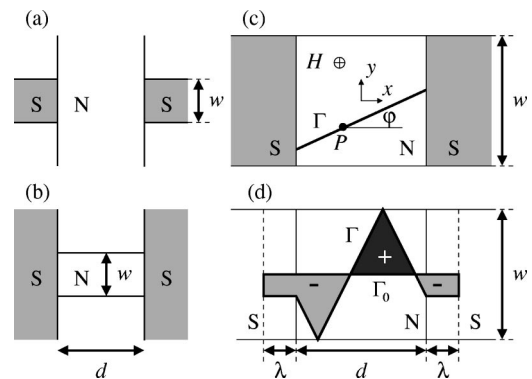


FIG. 1. (a) Junction with a point-contact (open) geometry as discussed in Ref. 10, where w is the width of the two superconductors. (b) The junction studied here has a strip geometry with w the width of the normal conductor. (c) The magnetic field H is applied in the z direction and the coordinate system is chosen symmetric with respect to the junction center. The current density in the point P involves contributions from all trajectories Γ parametrized by the angle φ . (d) The phase difference γ along the trajectory Γ can be expressed through the enclosed flux ϕ ; using the trajectory Γ_0 as our reference, the flux through the areas above (below) Γ_0 contributes with a positive (negative) sign.

results from contributions over all *trajectories* of quasiparticles connecting one interface to the other through P . In a junction of infinite width, all trajectories go straight through the junction. In the case of a finite junction, boundary conditions at the normal-metal–vacuum boundary have to be applied, which we idealize through the assumption of specular reflections. Furthermore, we adopt the usual approximations: perfect Andreev reflections at the SN interfaces and a coherence length ξ_0 in the two superconductors with $\xi_0 \ll d$, allowing for a steplike approximation of the order parameter Δ .^{1,7,13} The quasiclassical Green's function is calculated by matching the partial solutions in N and S at the interfaces. For the current density \mathbf{j} , we arrive at a generalization of the results of Antsygina *et al.*⁷ Explicitly, for finite temperatures with $d \gg \xi_N$, \mathbf{j} takes the form,

$$\frac{\mathbf{j}(x,y)}{j_{c,T}} = \frac{-1}{\sqrt{2\pi}} \int_{-\pi/2}^{\pi/2} d\varphi \hat{\mathbf{p}} \frac{\sin(\gamma)d}{\sqrt{\xi_N}l(\varphi)} \exp\left(\frac{d-l(\varphi)}{\xi_N}\right), \quad (1)$$

while in the low-temperature limit, $d \ll \xi_N$,

$$\frac{\mathbf{j}(x,y)}{j_{c,0}} = \frac{4}{\pi^2} \sum_{k=1}^{\infty} \frac{(-1)^k}{k} \int_{-\pi/2}^{\pi/2} d\varphi \hat{\mathbf{p}} \sin(k\gamma) \frac{d}{l(\varphi)}, \quad (2)$$

where $\hat{\mathbf{p}} = (\cos(\varphi), \sin(\varphi), 0)$, $l(\varphi) = d/\cos(\varphi)$ is the length of a trajectory with slope φ , and the critical current densities are

$$j_{c,T} = \rho j_{c,0} \exp\left(-\frac{d}{\xi_N}\right) \quad \text{and} \quad j_{c,0} = \frac{ne^2}{mc} \frac{\Phi_0}{2d}. \quad (3)$$

In Eq. (3), n denotes the electron density in the normal conductor and $\rho \approx 12/\pi$ for $T \ll T_c$, $\lim_{T \rightarrow T_c} \rho \sim 1 - T/T_c$. While in the low-temperature limit all harmonics $\sin(k\gamma)$ ($k=1,2,\dots$) contribute to the current density,¹³ at finite temperatures, thermal smearing of the Andreev levels leads to a suppression of the higher harmonics $\propto \exp(-kd/\xi_N)$ and only the first term $\propto \sin(\gamma)$ survives. An individual trajectory contributes with a weight $\propto \exp(-l/\xi_N)$ at finite- and $\propto d/l$ in the low-temperature limit. In a wide junction, γ takes the form,⁷

$$\gamma(x,y;\varphi) = \gamma_0 - \frac{2\pi}{\Phi_0} Hd' [y - x \tan(\varphi)]. \quad (4)$$

The more general expression derived here results in the gauge-invariant phase difference

$$\gamma(x,y;\varphi) = \Delta\varphi - \frac{2\pi}{\Phi_0} \int_{\Gamma} \mathbf{A} \cdot ds, \quad (5)$$

where $\Delta\varphi$ denotes the phase difference between the two superconductors and Γ is the path which goes through the point (x,y) with slope φ . Combining the current expressions (1) or (2) and (5) with the Maxwell equation $\nabla^2 \mathbf{A} = -4\pi \mathbf{j}[\mathbf{A}, \Delta\varphi]/c$, we obtain the transverse vector-potential \mathbf{A} and thus can solve the full screening problem; in the case of a tunnel junction (where the trajectories are reduced to the one with $\varphi=0$), numerical and analytic calculations have been given by Owen and Scalapino.¹⁴

In the following, we neglect screening and concentrate on junctions with the strip geometry of Fig. 1(b), including the (reflecting) trajectories Γ in Eqs. (1) and (2). We express the

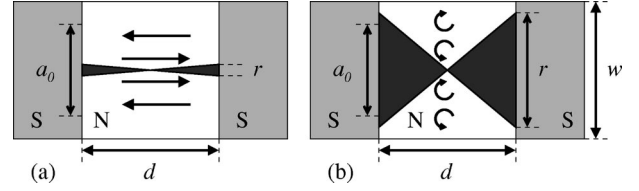


FIG. 2. The “bow ties” of width r display the ensemble of trajectories contributing to the current density in a given point. The arrows indicate the current flow. (a) For weak nonlocality, $r < a_0$, the current flows straight through the junction. (b) The strong nonlocality, $r > a_0$, leads to the formation of vortexlike domains of circular flow.

gauge-invariant phase difference (5) in terms of the flux ϕ enclosed by Γ and the reference path Γ_0 and obtain,

$$\gamma(x,y;\varphi) = \gamma_0 - \frac{2\pi\phi(x,y;\varphi)}{\Phi_0}, \quad (6)$$

where for negligible screening $\phi(x,y;\varphi) = H\mathcal{A}(x,y;\varphi)$ and \mathcal{A} is the properly weighted enclosed area, see Fig. 1(d). The area \mathcal{A} is calculated as a function of the number of reflections the trajectory Γ undergoes (in the following called the “order” of the trajectory). The point-contact geometry of Fig. 1(a) then is described by the order-zero trajectories alone,¹⁰ while in the strip geometry of Fig. 1(b), higher orders have to be included.

The geometrical pattern in the current density \mathbf{j} depends strongly on the sample dimensions d and w , the normal-metal coherence length ξ_N , and the applied field H . At finite temperature, the current density in P draws its weight from trajectories with $\varphi < \sqrt{\xi_N/d}$, allowing us to introduce the transverse nonlocality range $r = \sqrt{\xi_N d}$ (in the low-temperature limit, $\varphi \sim 1$ and we define $r = d$). This range of nonlocality has to be compared to the scale $a_0 = \Phi_0/Hd'$ of transverse variations in \mathbf{j} (see Fig. 2): For *weak* nonlocality, $r < a_0$, the flow is uniform along x with amplitude j_c and changes direction on a distance $a_0/2$ going up the y axis. This contrasts with the *strongly* nonlocal case $r > a_0$, where the current density forms domains of left and right going circular flow. While the local case is similar to that in a tunnel junction, the pattern in the *nonlocal* situation reminds of the usual vortex structure in a superconductor, see Fig. 3. Explicitly, for finite temperatures with $d \gg \xi_N$, the current density of the order-zero trajectories is given by

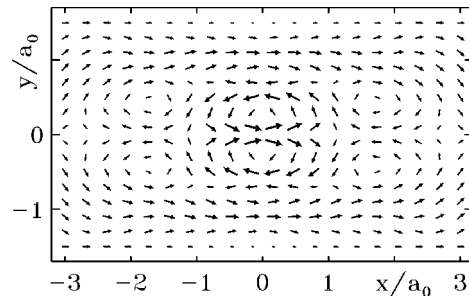


FIG. 3. The current density for $d/\xi_N=3$, $r/a_0 \approx 3.5$, and $\Phi/\Phi_0=3$. Apart from the vortexlike domains in the middle produced by order-zero trajectories, additional circular flow is set up by the order-one trajectories.

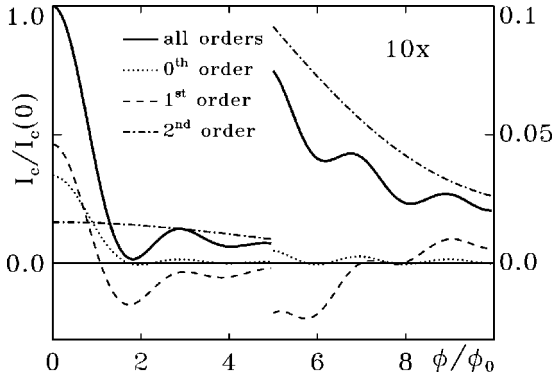


FIG. 4. The critical current for $d/\xi_N=5$ and $w/d=1/3$. The solid curve shows the full critical current and the dashed curves are the contributions from the orders 0, 1, and 2. The orders 0 and 1 oscillate with periodicity $2\Phi_0$, while the second order decreases monotonically, remaining always positive. The current pattern produced by the orders 0 and 1 is lifted by the order 2 contributions, and the critical current attains the periodicity $2\Phi_0$.

$$\frac{j_x(x,y)}{j_{c,T}} = -\sin\left(\gamma_0 - \frac{2\pi y}{a_0}\right) \exp[-\alpha(x)],$$

$$\frac{j_y(x,y)}{j_{c,T}} = -\cos\left(\gamma_0 - \frac{2\pi y}{a_0}\right) \frac{\xi_N}{d} \frac{2\pi x}{a_0} \exp[-\alpha(x)], \quad (7)$$

where

$$\alpha(x) = -\frac{d}{\xi_N} + \sqrt{\left(\frac{d}{\xi_N}\right)^2 + \left(\frac{2\pi x}{a_0}\right)^2}. \quad (8)$$

For weak nonlocality, $a_0 < r$, the exponent remains approximately constant in the normal part, $\alpha(x) \approx \alpha(0)$, leading to a uniform current flow, while for strong nonlocality, $a_0 > r$, $\alpha(x)$ grows as x approaches the interfaces, $\alpha(\pm d/2) \gg \alpha(0)$, such that the current concentrates in the middle of the junction. For $a_0 > r$, the higher order trajectories lead to a refinement of the current pattern, see Fig. 3 (similar results are obtained in the low-temperature limit).

The ratio r/a_0 and its associated characteristic current pattern manifest themselves in the (pseudo)periodicity of the critical current,

$$I_c(\Phi) = \max_{\gamma_0} \int_{-w/2}^{w/2} dy j_x(0,y; \gamma_0, \Phi), \quad (9)$$

versus flux $\Phi = Hd'w$ in the junction. In the case of weak nonlocality, $r < a_0$, the relevant contribution to the critical current comes from the order-zero trajectories resulting in a Φ_0 periodicity. For strong nonlocality, $r > a_0$, higher orders are relevant and *lift* the order-zero result as shown in Fig. 4 — the periodicity of the critical current changes to $2\Phi_0$ (the crossover lies within the negligible screening regime if $j_c < \phi_0/cd^3$). To be specific, we discuss in detail the orders 0, 1, and 2 for the case of finite temperatures with $d \gg \xi_N$ (the qualitative arguments for $d \ll \xi_N$ are similar).

For $w > r > a_0$, the critical current due to the order-zero trajectories takes the form,¹⁵

TABLE I. The periodicity of the critical current is controlled by the three parameters w/d , w/r , and r/a_0 . The table has to be read as a flow chart, starting at the top row and selecting the proper condition proceeding down the rows. Note that always $w/d < w/r$.

ratio	value		
w/d	> 1	< 1	$\rightarrow 0$
w/r	> 1	< 1	
r/a_0	< 1	> 1	
period	Φ_0	$2\Phi_0$	none

$$I_c^{(0)}(\Phi) = -\frac{\sqrt{2}I_{c,T}}{\sqrt{\pi}} \frac{w}{r} \frac{\cos(\pi\Phi/\Phi_0)}{(\pi\Phi/\Phi_0)^2}, \quad (10)$$

where $I_{c,T} = wj_{c,T}$. For the first-order trajectories, we numerically find again a $2\Phi_0$ (pseudo)periodic contribution. Both components vanish with field $\propto 1/\Phi^2$. The second- and all following even-order trajectories exhibit a large current amplitude of order j_c on a scale $a_0 \propto 1/\Phi$ in the junction center (0,0), a consequence of the φ independence of the gauge-invariant phase difference γ along trajectories through (0,0). Their contribution scales $\propto 1/\Phi$ and therefore dominates over the zeroth- and first-order terms at large enough fields — as the strongly nonlocal limit with $a_0 < r$ is reached, the periodicity changes over to $2\Phi_0$. Samples with a small width $w < r$ are always in the strongly nonlocal limit and their current pattern is $2\Phi_0$ periodic throughout the entire field axis. At low temperatures, the condition $w < r$ transforms into the geometric requirement $w < d$. In the very limit $w/d \rightarrow 0$ the periodic modulation disappears and the solution goes over into the zero-field result, $I_c(\Phi) \rightarrow I_c(0)$. The complete classification is given in Table I.

Recently, Heida *et al.*⁹ observed such a $2\Phi_0$ periodicity in striplike ($w \sim d$) S-2DEG-S junctions made from Nb electrodes in contact with InAs operating at low temperatures $T=0.1$ K (similar junctions have been constructed by Takayanagi *et al.*, see Ref. 8). As the total flux through the junction is difficult to determine in the experiment, Heida *et al.* had to infer their $2\Phi_0$ periodic structure from a fit on four samples with different ratios w/d ranging from 0.9 to 2.2.

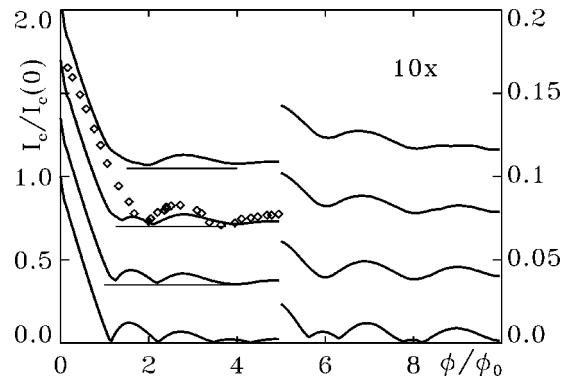


FIG. 5. The critical current in the low-temperature limit, $d \ll \xi_N$, for $w/d=0.8, 0.9, 1.1, 1.5$ (from top to bottom). Successive plots have been offset by 0.35. Measured data (Ref. 9, diamonds) are shown for the case $w/d=0.9$.

In Fig. 5, we present the results of our numerical calculations for the strip geometry, where we have properly taken into account the finite penetration depth of the flux into the superconducting banks. While geometries with $w/d < 1$ clearly exhibit a $2\Phi_0$ periodicity throughout the entire field region, a Φ_0 -component starts to develop at low fields in wide junctions. The comparison with the data of Heida *et al.* ($w/d = 0.9$) gives a satisfactory description of the pseudoperiodic structure.

In conclusion, we have demonstrated that the current density and the critical current in a clean SNS junction with strip geometry depend crucially on the ratio r/a_0 between the nonlocality range r and the vortex distance a_0 . The period of

the critical current depends not only on the dimensions of the junction and the normal-metal coherence length ξ_N , as it is the case in a point-contact geometry,¹⁰ but also on the applied magnetic field H . In particular, we obtain a $2\Phi_0$ periodicity in the whole current pattern at $w \sim d$, whereas for a point-contact geometry, the $2\Phi_0$ periodicity is reached only in the limit $w/d \rightarrow 0$.¹⁰ The numerical results for the strip geometry are in agreement with the experiment of Heida *et al.*⁹ For wider junctions, we predict a crossover from a Φ_0 to a $2\Phi_0$ periodicity at high fields.

We thank D. Agterberg and V. Geshkenbein for stimulating discussions throughout this work.

¹I.O. Kulik, Zh. Éksp. Teor. Fiz. **57**, 1745 (1969) [Sov. Phys. JETP **30**, 944 (1970)].

²A.D. Zaikin, Solid State Commun. **41**, 533 (1982).

³W. Belzig, C. Bruder, and A.L. Fauchère, Phys. Rev. B **58**, 14 531 (1998).

⁴B.D. Josephson, Phys. Lett. **1**, 251 (1962).

⁵K.K. Likharev, Rev. Mod. Phys. **51**, 101 (1979).

⁶A.F. Andreev, Zh. Éksp. Teor. Fiz. **46**, 1823 (1964) [Sov. Phys. JETP **19**, 1228 (1964)]; **49** 655 (1965) [**22**, 455 (1966)].

⁷T.N. Antsygina, E.N. Bratus, and A.V. Svidzinskii, Fiz. Nizk. Temp. **1** 49 (1975) [Sov. J. Low Temp. Phys. **1**, 23 (1975)].

⁸H. Takayanagi, J.B. Hansen, and J. Nitta, Phys. Rev. Lett. **74**, 166 (1995); H. Takayanagi, T. Akazaki, and J. Nitta, *ibid.* **75**, 3533 (1995).

⁹J.P. Heida, B.J. van Wees, T.M. Klapwijk, and G. Borghs, Phys. Rev. B **57**, R5618 (1998).

¹⁰V. Barzykin and A.M. Zagoskin, cond-mat/9805104 (unpublished).

¹¹M. Tinkham, in *Introduction to Superconductivity*, 2nd ed. (McGraw-Hill, Singapore, 1996).

¹²G. Eilenberger, Z. Phys. **214**, 195 (1968).

¹³C. Ishii, Prog. Theor. Phys. **44**, 1525 (1970).

¹⁴C.S. Owen and D.J. Scalapino, Phys. Rev. **164**, 538 (1967).

¹⁵In the opposite case $r > w > a_0$, we are in the limit $w/d \rightarrow 0$, where the order-zero critical current is given by the result conjectured in Ref. 9.